B cell αv integrin regulates germinal center derived lung-resident IgA B cell responses following influenza virus infection.

Andrea Montiel-Armendariz[1]†, Kelsey Roe[1]†, Jonathan Lagos-Orellana[1], Laura Veronica Martinez-Castro[1], Adam Lacy-Hulbert[2] and Mridu Acharya[1,3]*

[1]Seattle Children's Research Institute, Seattle, WA

[2]Benaroya Research Institute, Seattle, WA

[3]Department of Pediatrics, University of Washington, Seattle, WA

†AMA and KR contributed equally to the manuscript.

*Corresponding author:

Mridu Acharya, Seattle Children's Research Institute, Seattle, WA, USA

Telephone: (206) 884 2349

Mridu.acharya@seattlechildrens.org

Abstract

Emerging studies have highlighted the importance of tissue-resident B cells in the lungs for protective immunity against respiratory viruses. However, mechanisms controlling maintenance of B cell responses at respiratory sites such as lungs remain obscure. We have previously shown that the αv family of integrins limit B cell responses to antigens containing Toll-like receptor ligands, therefore deletion of B cell αv integrins in mice, enhances long-lived B cell responses against viral antigens, after systemic immunization. Here, we investigated whether αv can also regulate B cell responses at the respiratory tract, during viral infection. Our data show that αv integrin restricts development of lung-resident B cells and loss of B cell αv promotes generation of lung-resident IgA B cell responses following influenza A virus (IAV) infection of mice. Analysis of infection induced B cells in the lungs showed that loss of B cell αv promotes persistence of germinal center (GC) reactions locally in the lungs, leading to increases in lung-resident IgA+ GC and memory B cells, cross-reactive to antigenic variants. Thus, these studies reveal how IgA B cells are maintained in the lungs and point to a new strategy to improve the durability of lung-resident B cell responses for IAV vaccine efficacy.

Introduction

B cells are crucial in mediating immune responses against rapidly mutating pathogens, such as mucosal respiratory viruses, human immunodeficiency virus (HIV), and malaria, as they can generate antibodies of varying affinities and changing reactivities that can target mutation induced antigenic variants. Furthermore, long-lived plasma cells and memory B cells can provide long-term protection against re-infection from the same pathogen or antigenic variants of the pathogen. B cells can also induce short-lived antibody responses that provide rapid early protection against multiple pathogens that initiate acute early pathologies. B cells encounter antigen through their B cell receptor (BCR), which leads to B cell activation and differentiation. Activation of other receptors by molecules associated with the antigens, further modifies the strength of B cell activation. For example, the Toll-like receptors (TLRs), a family of innate immune receptors expressed on multiple B cell subsets, can modify B cell responses in the context of the antigen encountered. TLR ligands are integral components of both products from pathogens or self-antigens, and therefore TLRs are involved in both protective immunity as well as in self-reactive B cell responses in autoimmunity. B cells can receive signals from TLR ligands alone, which lead to rapid short-lived antibody responses. Stimulation of the TLRs together with BCR signals can promote GC-dependent B cell responses associated with affinity maturation of antibodies and development of long-lived memory B cells and plasma cells[1]. Understanding signals that modulate B cell responses through multiple receptor families could allow us to fine-tune B cell responses in autoimmunity and promote protective immune response against multiple pathogens.

αv integrins are a family of integrins with diverse roles in multiple immune cell populations, such as dendritic cells, macrophages, T cells, and B cells[2-9]. In previous studies, we described a new mechanism of regulation of B cell responses by the αv family of integrins. Specifically, we found that B cell stimulation by TLR ligands activates αv signaling on B cells and αv limits B cell TLR signaling, by promoting recruitment of the autophagy proteins to TLR-containing endosomes and regulating the duration and quality of TLR signaling[10]. Thus, $\alpha v^{-/-}$ B cells show increased signaling, proliferation and antibody production in response to TLR ligand stimulation (including stimulation with TLR4, TLR7 and TLR9 ligands) *in vitro* and *in vivo*[10]. As a result, B cell-specific $\alpha v^{-/-}$ mice show increased antibody responses after immunization with antigens associated with TLR ligand adjuvants, such as LPS (TLR4 ligand)[10] or Imiquimod (TLR7 ligand)[11]. Loss of B cell αv does not alter B cell responses to B cell receptor/CD40 stimulation and B cell specific αv conditional knockout mice mount normal primary and secondary antibody responses to immunization with a T cell-dependent (TD) antigen in alum adjuvant[10]. Thus, B cell αv integrin specifically regulates TLR stimulation related B cell functions. Although αv forms 5 different integrin heterodimers, this TLR related role is mediated primarily by αvβ3[10, 12]. This regulatory role of αv limits self-reactive B cell responses in the context of autoimmunity and loss of B cell αv integrins accelerates development of autoimmunity in mouse models of TLR ligand driven autoimmunity[13]. However, this loss of αv from B cells is beneficial in the context of immune responses to viral antigens. In previous studies, we showed that loss of B cell αv from mice leads to increase in germinal center derived antibody response, memory B cells and long-lived plasma cells, after immunization with TLR ligand containing virus like particles. More importantly, loss of B cell αv led to increases in somatic hyper mutation (SHM) of antibodies relevant for changing the affinity and breadth of reactivity of antibodies. These changes in B cell responses were particularly beneficial for development of protective immunity against influenza virus, as mice lacking B cell αv integrins developed more cross-reactive antibodies after systemic immunization with a single strain. B cell specific αv knockout mice also showed better protection during infection with influenza virus[11]. These changes in the B cell

specific αv knockout mice were associated with specific increases in antigen directed responses, indicating blockade of αv could be beneficial to drive protective B cell responses for antiviral immunity. In the context of antiviral immunity, emerging studies have highlighted the importance of mucosal and respiratory B cell responses in development of protective immune response against respiratory mucosal viruses, such as influenza. Therefore, we were interested to know whether this role of αv in regulating B cell TLR responses could also be relevant to regulate mucosal B cell responses during infection with respiratory viruses.

Multiple cell types orchestrate immune responses in the lungs during viral infection and recent studies point to a critical role for the lung-resident B cells in this process. For example, antigen-specific lung-resident memory B cells elicited by viral infection have been shown to be critical for protection against secondary infection[14]. Another study showed that these lung-resident memory B cells are of IgA isotype and differentiate to produce the mucosal immunoglobulin, IgA, which possesses unique characteristics for mucosal immunity. This study also showed that intranasal immunization leading to respiratory tract IgA provides better protection during challenge with influenza virus compared to systemic immunization, which does not generate strong respiratory tract IgA[15]. This was shown in the setting of T cell depletion, indicating a B cell specific role for protection. Mucosal IgA antibodies secreted by B cells which have class switched to IgA (IgA+ B cells) and differentiated into plasma cells, are a key component of mucosal immunity. Secreted IgA can be transported across the mucosal barrier by epithelial cells, providing unique opportunities to neutralize pathogens on the mucosal surfaces[16-18]. While knockout mouse studies show that IgA is not essential for protection against Influenza infection, multiple studies have shown the capacity of mucosal IgA to provide protection from infection and pathology, in animal models [15, 19-21]. Generation of IgA B cell responses has been well studied in the gut mucosa, but the mechanisms driving IgA B cell responses in the lung are still not clear. Thus, despite multiple evidence showing the importance of these IgA B cells in protective immune response at the respiratory tract, it is still not clear how they are maintained in the lungs and therefore there is a lack of strategies to drive these responses through vaccines. Based on the increased GC derived IgG antibody responses seen after systemic immunization, in the B cell specific αv knockout mice and the increase in protection seen in these mice after influenza virus infection, we asked whether B cell αv integrin could also regulate GC related IgA and memory B cells in the lungs during viral infection.

Our data showed that αv integrin restricts development of lung-resident B cells after infection, through its B cell intrinsic role on processing of TLR signaling. Loss of B cell αv leads to increase in lung-resident IgA isotype B cells after influenza infection which is driven by the persistence of GC reactions occurring in the lungs and results in increases in IgA GC and memory B cells that are cross-reactive to antigenic variants of infecting virus. These data firstly clarify that IgA B cell responses can be generated through GC reactions occurring in the lungs and secondly show that blockade of B cell αv could be a way to promote long-lived GC derived IgA antibody responses for protective immunity against respiratory viruses such as influenza.

Results

Generation of cross-reactive B cell responses in the lungs is regulated by B cell αv integrin.

We have previously demonstrated that loss of αv integrin from B cells promotes TLR signaling driven, GC -dependent antibody responses against viral antigens. Using immunization with influenza antigens, we also demonstrated that this increase in GC related antibody response leads to an increase in cross-reactive

antibodies in mice after immunization[11]. Moreover, these studies also demonstrated that mice lacking the αv integrin on B cells, the αv conditional knockout mice survive better during influenza A virus (IAV) infection than their wild-type counterparts, which led us to ask whether αv integrin has a role in regulating B cell responses directly in the lungs during infection.

We therefore investigated the generation of IAV-specific B cells in the lung and the draining mediastinal lymph nodes (medLN), following low dose intranasal IAV infection in control and the B cell specific αv conditional knockout mice (referred to as cKO mice) (**Figure 1A**). We infected mice with a sub-lethal dose of H1N1 PR8 IAV and 14 days later looked for the presence of B cells that recognized PR8-HA, as well as cross-reactive B cells to the HA from the pandemic H1N1 California2009 (Cal09) IAV strain by using ELISpot assay. Quantification of IgG-secreting cells (IgG-ASCs) by ELISpot revealed that, following PR8 IAV infection, cKO-infected mice had higher numbers of PR8-HA-specific IgG-ASCs in the lung, as compared to the control mice (**Figure 1B, left**). However, this increase was more pronounced when we measured the numbers of IgG-ASCs that recognized Cal09 HA (**Figure 1B, right**). Hence αv integrins can regulate cross-reactive IgG B cell responses induced in the lungs by viral infection, as we had seen with systemic immunization.

To identify B cell subpopulations associated with the increases in cross-reactivity in the lungs of cKO mice, we injected mice with an α-CD45 antibody in the retro-orbital cavity five minutes prior to euthanasia and used flow cytometry to identify cells that were in the lung parenchyma (cells identified as being i.v. $CD45^-$) (**Sup Figure 1 and 2A**). At day 14 after IAV infection we found a population of lung-resident B cells with a germinal center (GC) phenotype (Fas^+, PNA^+). Using tetramers that recognize antigen specific cells induced by infection (**Sup Figure 2B**), we identified similar numbers of PR8-HA-specific cells in the cKO mice, compared to controls, within this GC population (**Sup Figure 2C**). However, we found significantly more cells with the GC phenotype that were lung-resident and recognized Cal09-HA in the cKO mice (**Figure 1C, left**). Similarly, we found more Cal09-HA specific class-switched lung-resident memory B cells (Sw Mem B cells) in the absence of B cell αv integrin (**Figure 1C, middle**). Conversely, while both strains of mice induced PR8 and Cal09-specific lung-resident IgM^+ Mem B cells after IAV infection, there was no difference observed between cKO and control mice (**Figure 1C right and Sup Figure 2C right**). This increased cross-reactivity of B cells in the cKO mice following IAV infection, was specific to the lungs; Cal09-HA-specific cells were found in the medLN and were increased following IAV infection. However, there was no difference in the numbers of Cal09 specific IgG producing cells or in the percentage of Cal09 specific GC and memory B cells, in the presence or absence of B cell αv integrin (**Sup Figure 3**). These data therefore indicate that B cell αv integrin regulates generation of cross-reactive B cells in the lungs following infection and this effect of αv is an attribute related to the lungs.

Absence of B cell αv integrin increases the proportion of IgA^+ cells in the lungs of influenza infected mice.

Given the importance of the IgA isotype in protective pulmonary immunity, we next asked whether αv integrin on B cells also regulated the development of IgA isotype B cells, following IAV infection. Therefore, we assessed IgA isotype B cells in the lungs of PR8-infected mice at day 14, post infection. As with IgG, we found that the cKO mice had slightly higher numbers of PR8-sepcific IgA-secreting cells, compared to control mice (**Figure 2A, left**). These mice also had significantly more IgA ASCs that recognized the heterologous Cal09 strain (**Figure 2A, right**). This suggests that the expanded cross-reactivity observed in the absence of αv integrin is independent of the Ig isotype expressed by the B cells and that αv regulates generation of cross-reactive IgA B in the lungs following infection.

IgA isotype B cells can be generated at mucosal surfaces through short-lived or long-lived B cell responses[22] . Therefore, we examined IgA+ lung-resident B cells by flow cytometry to identify the cellular lineage that gave rise to the increases in IgA-secreting ASCs in the cKO mice after infection. We again used CD45 i.v. antibody labeling prior to euthanasia, to identify lung-resident B cells. Gating on the lung-resident (i.v. $CD45^-$) B cell population, we observed a small population of IgA^+ B cells within the GC B cell compartment, suggesting some of the IgA ASCs were derived from GC reactions. Importantly, we found significantly higher numbers of lung-resident IgA^+ GC B cells in cKO mice (**Figure 2B-C**). We also found higher numbers of lung-resident IgA+ PCs (plasma cells) (**Figure 2D-E**) and IgA^+ Mem B cells (**Figure 2F-G**) in the cKO mice, compared to control mice. These changes were induced by infection in the cKO mice as the numbers of IgA B cells were increased post infection when compared to IgA B cells in the lungs of mice without infection. Comparison of these lung-resident i.v. $CD45^-$ B cells, with i.v. $CD45^+$ circulating cells, further clarified that the cKO mice show specific increases in lung-resident IgA B cells of GC, memory and plasma cell phenotype. These comparisons also highlighted that while IgA negative B cells were distributed equally in the circulating and lung-resident compartments, majority of the IgA+ GC and memory B cells were lung-resident (**Sup Figure 4A-E**). Analysis of IgA+ GC cells in the lungs and medLN further showed that IgA+ GC cells were found mainly in the lungs (**Sup Figure 4F**). Moreover, comparison of IgA and IgG secreting cells in the lungs and medLN also confirmed that IgA secreting cells were found in the lungs and not in the lymph nodes and the increases seen in the cKO mice were mainly in the lungs (**Sup Figure 4G-H**). Thus, these data suggest that IgA isotype B cells are primarily lung-resident and can be related to GC reactions in the lungs. αv integrin on B cells modulates the generation of these lung-resident IgA isotype B cells, such that in its absence, more IgA B cells develop within the GC, memory, and plasma cell compartments in the lungs.

B cell αv integrin regulates persistence of GC reactions and development of lung-resident IgA memory B cells.

Germinal center reactions generally peak around day 14 after infection and our data indicated that loss of αv promotes cross-reactive and IgA isotype B cell responses in the lungs, after infection, around the peak of GC reactions. We were curious whether these increases in B cell responses in the cKO mice were sustained over time. To answer this, we infected mice intranasally with a sub-lethal dose of PR8 IAV and used the i.v. CD45 antibody labeling to analyze the proportion of lung-resident i.v. $CD45^-$ B cells, by flow cytometry at day 35 post infection (**Figure 3A**). Interestingly, we found that at day 35 post infection, cKO mice showed a significant increase in the percentage of lung-resident B cells with GC B phenotype (**Figure 3B**). Within this GC compartment, we were able to identify a small percentage of IgA-expressing B cells which were mainly present in the cKO mice and not in the controls (**Figure 3B middle**). For previous analysis of antigen specific cells (**Figure 1 and Sup Fig 2**) we used linear HA probes which may not identify all antigen specific cells. Therefore to identify majority of antigen-specific cells, we also obtained conformationally intact HA tetramers that have been disabled for sialic acid binding and have been used in other studies to identify influenza antigen-specific and cross-reactive B cells[23, 24]. We verified that these tetramers could be used to identify antigen-specific cells. We could also identify a small number of cross reactive Cal09-HA specific cells after PR8 infection, using these tetramers. (**Sup Figure 5A**). Analysis of PR8-HA and Cal09-HA specific B cells within the lung-resident GC compartment at day 35, showed that while the percentage of HA-specific cells was small, the cKO mice still showed a detectable increase in antigen specific (PR8-HA+) or cross-reactive (Cal09-HA+) GC cells (**Figure 3B far right**). We also found that the cKO mice had a significant increase in the percentage of lung-resident class-switched Mem B cells and

IgA+ Mem B cells, compared to the controls (**Figure 3C**). Similar to HA-specific GC cells, we found a small percentage of PR8-HA specific Mem B cells and IgA MemB cells, present only in the cKO mice (**Sup Figure 5B**) and there was a very low percentage of Cal09-HA+ Mem B cells in mice of both genotype at this time point (**Sup Figure 5C**). The overall frequency of plasma cells was also low at this time point; however, we still detected a slight increase in IgA PCs in the cKO mice, compared to the controls (**Figure 3D**).

As the frequency of HA specific B cells at 35 days post infection was low, we performed a cluster analysis to better understand the connection between antigen specificity and lung-resident IgA B cells (**Figure 3E**). Using the Cytofkit package from Biocunductor[25]**,** we performed a PhenoGraph clustering analysis, and identified 11 clusters within the HA-specific lung-resident IgD- B cell phenotypes based on the makers used for flow cytometry staining. We found 4 of these clusters (11, 4, 2 and 7) had a higher frequency of cells in the cKO mice, compared to controls. Interestingly, these 4 clusters showed both higher IgA expression and increased staining for Cal09-HA, compared to other clusters (**Figure 3E**). Moreover, these 4 clusters also showed increased expression of GC-associated markers (Fas and PNA), compared to other clusters (**Figure 3E**). On the other hand, the clusters that had a higher frequency in the control mice compared to the cKO (cluster 6, 9, and 8), had an increased PR8-HA and IRF4 expression (**Figure 3E**), markers associated with plasma cells recognizing the infecting strain of IAV. Thus, loss of αv promotes the generation of IgA isotype B cells that are associated with the GC compartment and show increased cross-reactivity.

To address antigen specificity of lung-resident memory B cells, we re-challenged mice at day 31 of infection, as we predicted this would lead to expansion of antigen-specific memory B cells and provide enough cells for analysis. We analyzed memory B cells at day 4 post re-challenge, when the memory response should be at peak. Cluster analysis of lung-resident memory B cell indicated that clusters showing increased frequency of cells in the cKO mice (cluster 8, 1, 6 and 7) were highly positive for Cal09-HA and the marker CD73 **(Figure 3F)**. There was only one cluster showing high IgA expression (cluster 8), which was one of the clusters with increased frequency of cells in the cKO mice and showed high CD73 expression as well as increased staining for Cal09-HA. CD73 is a marker associated with GC derived memory B cells[26], therefore these findings indicate that loss of B cell αv promotes sustained increase in GC driven cross-reactive IgA memory B cells in the lungs, after infection with influenza. Together, these data suggests that αv deletion on B cells leads to a prolonged germinal center response in the lung upon intranasal infection with influenza virus, and that this germinal center reaction drives an increase in IgA memory B cells cross-reactive to antigenic variants of the antigen from the infecting virus.

Loss of B cell αv integrin promotes infection induced GC reactions locally in the lungs.

To confirm that the changes in lung-resident B cell responses seen in the cKO mice were due to immune reactions occurring in the lungs, we performed immunofluorescence analysis of B cells in the lung tissue, isolated from mice at day 16 post infection (**Figure 4A**). The generation of inducible bronchus-associated lymphoid tissues (iBALT) in the lungs after influenza infection, has been previously described and these structures are known to be associated with GC cells[27, 28] . Therefore, we hypothesized that the increased B cell responses in the cKO mice could be associated with iBALT structures in the lungs and we investigated whether the cKO mice have, either an increased number or better defined iBALT associated GC structures in the lungs, compared to the lungs from control mice. Furthermore, based on our flow cytometry analysis, we predicted that the germinal centers of the cKO mice could also have increased amount of IgA+ cells.

We first compared IgA+ cells in the lungs of cKO and control mice, by capturing a 1mm x 1mm portion of one lobe of the lung. Confirming our flow cytometry data, we found that the cKO mice lungs showed an increase in IgA+ cells, compared to the controls at 16 days after infection (**Figure 4B**). Next, we wanted to know if the cKO mice had an increased number of GCs, or if the GC structure would be bigger and better defined when compared to the control lungs after infection. We used GL7 to mark GC cells (**Supp Fig 6**) and used CD19 staining for B cells. We captured multiple sections of 1mm x 1 mm and identified the areas where GL7+ B cells clustered together and defined these as iBALT areas with GC cells. We found that iBALT regions were close to airway structures in both groups. We also noticed that the cKO mice had bigger iBALT GC areas, compared to the lungs from control mice (**Figure 4C and D**). Quantification of these iBALT GC areas or of GL7 staining within these areas both showed that iBALT-like structures with GC cells were predominantly larger and more distinct in the lungs from cKO, compared to the lungs of the control mice (**Figure 4E-F)**. Finally, to assess the contribution of GC reactions to IgA B cells, we quantified the area of IgA+ cells within the iBALT areas and also calculated colocalization of IgA and GL7 within the iBALT (**Figure 4D and G-H**). We found that the area of IgA+ cells within the iBALT was increased in cKO mice compared to the control group (**Figure 4G**) and there was also an increase in colocalization of IgA+ and GL7+ cells in the cKO mice compared to the control mice (**Figure 4H**). These data indicate that loss of B cell αv promotes the generation of GC reactions the lungs which contain IgA isotype B cells.

To confirm the persistence of these iBALT structures and GC cells, we performed similar analysis at day 35, post infection. At day 35 post infection, we continued to see increases in IgA+ cells in the lungs from cKO mice (**Figure 5A**). At this time point, iBALT-GC areas in lungs from both control and cKO mice had a similar size. However, GL7 staining intensity within these areas was clearly higher in the lungs from cKO mice (**Figure 5B-D**), indicating continued persistence of more distinct GC clusters in the lungs of cKO mice. We also found that both the area of IgA+ cells (**Figure 5E**) and the colocalization of IgA and GL7 (**Figure 5F**) within the iBALT-GC structures continued to be higher in the cKO mice compared to the control. Together, these data confirm that loss of B cell αv promotes the generation and persistence of GC reactions locally in the lungs, and thus results in increases in lung-resident IgA GC and memory B cells.

B cell αv integrin regulates IgA class-switch recombination in a B cell intrinsic manner

To further investigate the mechanism by which αv integrin is affecting class-switching to IgA isotype, we adapted an *in vitro* culture system, previously described[29, 30] to drive the differentiation of naïve B cells into IgA isotype plasma cells, using retinoic acid and the cytokine TGFβ. These cultures are not designed to promote differentiation of GC B cells, but they allow us to assess the differentiation of B cells into more activated B cells and antibody producing plasma cells. We used TLR9 ligand stimulation in these differentiation cultures to activate B cells and drive efficient plasma cell differentiation. This allowed us to also assess whether the regulation of TLR signaling by the αv integrin on B cells is involved in regulation of IgA B cell differentiation. We used total B cells sorted from either lung (i.v.CD45$^-$ lung-resident), spleen or medLN for the assay and after 8 days of culture, the phenotype of the cells was analyzed by flow cytometry (**Figure 6A**).

We found that cultures from cKO B cells led to an increased percentage of IgA isotype plasma cells (IRF4+ cells) from both the spleen and lungs, compared to cultures from control mice (**Figure 6B-D**). However, we noted that the fold increase of IgA+ B cells from the cKO vs the control was significantly higher in the lung B cell cultures compared to cultures from spleen B cells, indicating the importance of lung microenvironment in shaping IgA B cell response(**Figure 6C**). Furthermore, we found that cultures of B

cells from medLNs also led to development of IgA isotype plasma cells, but the fold change between cKO and control cultures was very small. The observed increase in the frequency of IgA B cells was related to the differentiation of lung B cells in culture, as we could see an increase in IgA-expressing B cells in the cultures compared to the percentage of IgA-expressing B cells at basal levels from the same mice (**Figure 6D**). Analysis of the culture supernatant by Enzyme-linked immunosorbent assay (ELISA), also confirmed an increase in IgA antibody secretion in the cKO lung B cell cultures, compared to the control (**Figure 6E**).

To confirm whether this increase in differentiation of IgA isotype B cells in the cKO cultures is indeed related to TLR stimulation, we investigated differentiation of lung B cells into IgA isotype B cells with TLR stimulation alone, replacing the activation step, feeder layer as well as retinoic acid and TGFβ with R848 stimulation alone during culture (**Figure 6F and G**). Overall, this condition produced less IgA-expressing B cells than cultures with feeder layers and retinoic acid and TGFβ stimulation, but flow cytometry analysis showed that R848 stimulation alone was sufficient to drive differentiation of IgA isotype lung B cells in culture, and this was increased in the cultures with lung B cells from cKO mice. (**Figure 6F**). Interestingly, we found that cultures from spleen B cells with R848 alone, did not significantly induce IgA differentiation (**Figure 6G**) again highlighting the advantage of lung B cells in IgA class switching. Thus, these data indicate that enhanced TLR signaling due to loss of B cell αv promotes increases in IgA B cell differentiation, and this effect is important in driving IgA B cell differentiation in the lung microenvironment.

Discussion

Recent studies have shown that natural infection of the respiratory tract by influenza virus induces memory B cells that are resident in the lung and are major producers of protective antibody IgA [14, 15]. These lung-resident cells are not generated by systemic immunization strategies and contribute significantly to the increased protection from secondary infection. Understanding the signals that regulate the generation of these lung-resident B cell populations will be critical to developing better intranasal immunization strategies to combat influenza and other mucosal respiratory viruses. Our data indicate that B cell αv integrin restricts lung-resident B cell responses, by regulating TLR signaling. Therefore, deletion of αv integrins from B cells promotes beneficial B cell responses in the lungs during viral infection. Loss of B cell αv promotes a sustained increase in GC reactions occurring locally in the lungs, which drive increases in cross-reactive IgA B cells and lung-resident memory B cells, after infection with influenza virus. Although we have previously shown a role for αv in promoting GC reactions after systemic immunization, the significance of these findings is that loss of B cell αv promotes GC reactions in tissue sites, such as the lungs, where it is difficult to induce such responses.

GCs are sites of affinity maturation of B cells, where B cells undergo successive rounds of proliferation, SHM and selection, through antigen presentation to T follicular helper (Tfh) cells[31]. Studies on influenza and other viral infections have revealed that affinity maturation through increasing SHM in the GCs not only increases the affinity of B cells and resulting antibodies to the immunizing antigen, but can also increase the breadth of responses to viral proteins, allowing generation of antibodies that can target multiple strains[32, 33]. We have previously shown that the absence of B cell αv integrins leads to increase in antigen- and TLR signal-induced GC reactions. As a result after systemic VLP vaccination, B cells from mice lacking B cell αv show increases in SHM in the IgG antibody heavy chain[11]. These studies also showed that after immunization with H1N1 PR8 strain, mice lacking αv on B cells exhibit increased antibody response to HA from the PR8 strain, as well as to the heterologous Cal09 strain, indicating higher levels of mutations in the αv-deficient B cells allowed them to expand the diversity of epitopes recognized. Thus, the increase

in antibody secreting cells, lung-resident GCs and memory B cells specific for Cal09-HA seen following PR8 IAV infection in the cKO mice, reported here, correlates with our previous findings and we predict this is related to the increased GC reactions occurring locally in the lungs. While we have not investigated cross-reactivity to further divergent influenza strains, based on the increase in GC reactions and SHM, we predict we would see an increase in the breadth of reactivity of antibodies produced in the lungs of cKO mice towards multiple antigenic variants of influenza virus. These results suggest that promoting GC reactions in the lungs and inhibiting B cell αv could be an important way to improve the breadth of B cell responses against antigenic variants of respiratory viruses, such as influenza, directly at the respiratory sites.

GC reactions are key for both affinity maturation of antibodies and the development of long-lived memory B cells and plasma cells and are therefore critical for protective immunity against multiple pathogens[34]. These reactions are known to be a prominent feature of secondary lymphoid organs especially lymph nodes. While GC structures had been described in the lungs after infection, the importance of these tissue-resident GC structures for protective immunity is still being established. Previous studies have shown that upon influenza infection, structures with similar compartmentalization and cellular composition to secondary lymphoid organs, termed iBALT, are ectopically generated in the lungs of mice and support GC B cell proliferation[28, 35]. Although the presence of iBALT in healthy adult humans has been controversial and may be associated with increased pathogenesis in respiratory tract diseases[36], a recent study has shown that these iBALT associated GC structures are present in lungs from children and are involved in respiratory virus immune response[27]. Thus, multiple studies suggest that antigen-derived iBALT development support B cell proliferation and maturation in the context of respiratory pathogens[37, 38]. However, mechanisms that promote such structures in the lungs are not clear, making it difficult to devise strategies to promote these through vaccination. Furthermore, it is not clear whether GC associated iBALT structures support the generation of IgA isotype B cells, and whether the majority of IgA memory B cells in the lungs are derived from GC reactions in the lungs. Our studies indicate that promoting these iBALT structures in the lungs could be the key to driving more durable IgA memory B cell responses against respiratory viruses.

We have previously shown that the loss of B cell αv enhances responses from innate B cell populations such as B1 B cells, Marginal zone B cells, as well as extrafollicular B cells[3, 13]. These B cell populations can all be involved in immune response against respiratory viruses[39] and likely lead to early IgA production at the respiratory tract. However, our data show a clear connection between IgA+ B cells and GC reactions in the lungs, related to more sustained IgA production in the absence of B cell αv. Flow cytometry analysis shows a relationship between IgA+ B cells, with GC markers, that are cross-reactive to Cal09-HA in the cKO mice at 35 days after infection (**Fig 3**). Moreover, our microscopy data clearly show an increase in GC structures and IgA+ B cells within these GC structures in the lungs of cKO mice, compared to the lungs from control mice (**Figs 4 and 5**). These data, together with the flow cytometry data showing that majority of IgA+ B cells are found in the lungs and are non-recirculating (**Fig 2** and **Sup Fig 4**), indicate that IgA+ GC and memory B cells are generated in the iBALT areas in the lungs, and deletion of B cell αv integrin can promote these B cells by sustaining GC reactions in the lungs. Lung-resident memory B cells in IAV infected mice are long lasting and require antigen encounter in the lungs for their generation, which links these memory B cells with GC reactions in the lungs[14, 40, 41]. After re-infection we find an increase in CD73+ IgA+ and Cal09-HA+ memory B cells. CD73+ memory B cells are thought to be GC-derived, and while we cannot rule out the possibility that these memory B cells could be generated from GC reactions in the medLN, based on our data demonstrating relative lack of IgA B cells in the medLNs (**Sup Fig 4**), we predict that the

increase in cross-reactive IgA memory B cells in the lungs of cKO mice are at least in part due to increased GC reactions in the lungs.

It is likely that influenza infection is also leading to increases in the IgG isotype B cells in the medLN and spleen in the cKO mice, which could contribute towards protective immunity. Here we have specifically focused on the IgA isotype B cells because the relevance of GC reactions in the development of IgA isotype B cells in respiratory sites, such as the lungs, is still not clear. IgA is the most common Ig isotype in the mucosal surface [42] and while multiple studies have suggested the importance of IgA antibodies in providing protection against respiratory virus infection, the mechanisms of generation and maintenance of IgA B cells in the respiratory tract remain unclear. TGFβ dependent mechanisms are known to be important for the generation of IgA B cells in subsets of germinal center B cells in the intestinal mucosa[43], but the role of TLR signaling in class switching to IgA isotype has not been clearly defined. While TLR signaling may not be a requirement for generation of IgA B cells, our data suggest that enhancing TLR signaling is enough to increase class switching to IgA isotype B cells, and this is particularly relevant for the B cells from the lung microenvironment. This could be related to specific aspects of B cells that have interacted with TLR ligand signals in lung mucosa. In previous studies, we have shown that loss of αv from B cells leads to increase in *Aicda* gene expression, related to TLR signaling[11, 12]. This increased expression could explain increases in both class-switching and SHM observed in the αv cKO B cells. It is also possible that increases in TLR signaling in the αv-deficient B cells allows for better antigen presentation and generation of memory B cells, as these cells require antigen encounter in the lungs[14]. It remains to be seen, however, why there is an increase specifically in class-switching to IgA in the lung. Our data suggest that the lung microenvironment itself influences this outcome, as naïve B cells from the spleen or medLN of the same mice do not share this propensity. Future studies are required to explore details of the mechanisms driving the generation of IgA isotype B cells in the lungs.

The increase in lung GC reactions in the cKO mice leads to questions about their functional capacity for protection. We observed a marked increase in CD73+ IgA memory B cells in the cKO mice, suggesting that these GC reactions results in an expanded memory response and thus likely confers better protection. Nonetheless, we were not able to address the contribution of IgA memory B cells in leading to protection after challenge studies, as we observed higher numbers of both IgG and IgA secreting cells in the lungs of cKO mice. Future studies are required to address the protective capacity of IgG versus IgA antibodies in driving protection and are beyond the scope of this study. However, our previous studies have demonstrated that the B cell specific αv knockout mice show better protection after a lethal intranasal infection, indicating the protective capacity of the lung-resident B cell responses in these mice[11]. Moreover, it has been proposed that HA-specific IgA, rather than IgG responses generated in the lung, are responsible for cross-strain protection from different IAV subtypes[44], indicating the key role of IgA antibodies in protection from respiratory mucosal viruses. Thus, we predict that the increased GC derived IgA responses in the cKO mice could play a major role in conferring superior protection compared to the IgG B cells in the event of a mucosal challenge. In further studies, we are exploring intranasal immunization strategies that would induce a similar expanded GC reaction in the cKO mice, which would allow us to harness the beneficial features of loss of B cell αv for vaccine studies.

Memory B cells capable of neutralizing multiple strains of the same pathogen have been identified in humans after influenza or HIV infection, but efforts to develop vaccines that induced broadly protective memory B cell response to pathogens have not yet been successful. Similarly, multiple recent studies have

shown the advantages of IgA inducing intranasal vaccines for blocking infection and transmission of respiratory viruses compared to systemic vaccines[15 45, 46]. But it has proven challenging to develop intranasal vaccines that lead to long-lived protection at the respiratory tract. Strategies that can promote GC reactions in the lungs could be beneficial to drive both broadly reactive and long-lived IgA memory B cells that are lung-resident and improve efficacy of intranasal vaccines. In this context, blockade of B cell αv could be used to improve efficacy of intranasal respiratory virus vaccines, as they could enhance multiple aspects of protective immune response against respiratory viruses, including, tissue-resident GC reactions, IgA isotype B cells, breadth of reactivity of B cells to evolving strains, and lung-resident memory B cell responses. Drugs and antibodies targeting the αv family of integrins have been tested therapeutically in other disease settings such as cancer, and therefore could be utilized for αv-blockade on immune cells. Thus, these studies using the B cell specific αv-deficient mouse model have allowed us to understand unique mechanisms in the lung microenvironment that control lung-resident IgA memory B cell responses and identified new strategies to promote immune responses directly at the respiratory tract for more effective respiratory virus vaccines.

Materials and Methods

Mice

$\alpha v^{fl/fl}$ mice were backcrossed to C57BL/6J mice as previously described[10, 11]. The animals were bred and maintained on the C57BL/6 background. $\alpha v^{fl/fl}$ mice were crossed with CD19 cre transgenic mice to generate B cell specific αv knockout mice, referred to as conditional KO (cKO) mice ($CD19^{cre/+}$ $\alpha v^{fl/fl}$). Mice with a single $CD19^{Cre}$ allele, $CD19^{cre/+}\alpha v^{+/+}$ were used as controls. For *in vitro* experiments C57BL/6 mice were used as controls. All mice for this study were age and sex-matched and were 9-14 weeks old at the time of infection or vaccination. Mice were housed in a specific pathogen-free facility. All procedures were approved by the Institutional Animal Care and Use Committee at Seattle Children's Research Institute.

Influenza infection

Live PR8 IAV was purchased from Charles River Laboratories and stored in one-use aliquots at -80°C. Just prior to infection, PR8 was thawed and diluted in PBS. Mice were anesthetized with Isoflurane (Patterson Veterinary) and infected with PR8 IAV in 25µL in the nostrils. Mice were weighed and monitored for signs and symptoms of disease for the duration of the study.

HA tetramer preparation

The B cell HA tetramers were either a gift from Dr. Emily Gage[47] or from Dr. Kanekiyo Masaru's lab at NIH. Tetramers with an AviTag were biotinylated with the BirA biotin-ligase kit (Avidity) according to manufacturer's instructions. Following biotinylation, BV711- (BioLegend) or PerCpCy5.5- (BioLegend) conjugated streptavidin was added in 5 serial steps with a 10-minute incubation period each to the unlabeled tetramers. Labeled tetramers were prepared the day before the experiment.

Antibodies

α-IgD-BV786, α-B220-BUV395, α-CD45-BUV395, α-CD19-BUV737 were purchased from BD Horizon. A-CD3-BV510, α-CD11c-BV510, α-F4/80-BV510, α-CD138-BV421, α-Fas-BV605, Streptavidin (SA)-

PerCPCy5.5, SA-BV711 and α-IgM-PerCPCy5.5 were from BioLegend. α-CD45-APC, α-IRF4-PeCy7 and α-IRF4-AF700 were purchased from Invitrogen. α-IgA-Biotin, α-IgA-PE and α-IgM-PeCy7 were from Southern Biotech. α-Gr1-BV510 and PNA-FITC were from Miltenyi Biotechnologies and Vector Labs, respectively.

Flow cytometry

5 minutes prior to euthanasia, mice were injected with 1µg α-CD45-BUV395 or α-CD45-APC in the retro-orbital cavity. Lungs and mediastinal lymph nodes (medLN) were collected from euthanized mice. Lung tissue was digested with 1.5mg/mL collagenase (Milipore Sigma) and 10µg/mL DNAse I (Milipore Sigma) in Mg^{2+}, Ca^{2+} free Hank's balanced salt solution (HBSS, Gibco) with 10% fetal bovine serum (FBS, Sigma) for 1 hr at 37°C or 30 min in a shaking incubator at 1000 rpm. Lungs and medLN were then ground into a 40µm filter to generate a single cell suspension. For some experiments lung B cells were isolated using CD19 positive magnetic bead separation (STEMCell). Cells were counted using AccuCheck count beads (ThermoFisher) or Muse Cell Analyzer (Luminex) according to the manufacturer's instructions. Cells were then stained with fixable LiveDead Aqua (ThermoFisher) to identify dead cells, after which cells were stained with PR8-HA and Cal09-HA B cell tetramers and surface antibodies for 20 minutes at room temperature. To identify intracellular antigens, cells were then fixed and permeabilized with a Transcription Factor kit (BioLegend) according to manufacturer's instructions. Events were analyzed on an LSRII flow cytometer (BD Biosciences) or an LSR Fortessa (BD Biosciences) and analyzed using FlowJo (v.10, TreeStar). See Supplemental **Figure 1** for gating strategies.

ELISpot

ELISpots were performed on single cell suspensions of lung or medLN cells, prepared as described above. MAIPS ELISpot plates (Millipore) were pre-coated with 3µg/mL PR8-HA or Cal09-HA (SinoBiological) diluted in PBS. Serial dilutions of cells were plated over wells and incubated over night at 37°C. Spots were developed using α-mouse IgG or α-mouse IgA alkaline phosphatase (AP) Abs (Southern Biotech) followed by BCIP/NBT AP substrate (Vectors Labs). Spots were imaged and counted using an ImmunoSpot analyzer (Cellular Technology Limited).

Histology and Immunofluorescence

Lungs were perfused with PBS and then inflated and embedded in OCT, and frozen at -80C (as described in[48]). Frozen sections (8µm) were fixed in acetone at -20C, air dried and blocked with 1% normal goat serum (Jacskon ImmunoResearch) and 1% BSA (Sigma) in PBS with 0.1% Tween-20 (Sigma). Slides were stained with Hoescht, α-CD19-AF647, α-GL7-FITC and α-IgA-PE. Images were acquired with a Zeiss LSM 900 confocal microscope. Image processing and analysis were performed with FIJI (ImageJ) software[49], with a personalized macro where the iBALT structure was manually delimited by the polygon tool, and then the image was converted to a mask by default threshold to measure the area of IgA and GL7 positive staining by the "analyze particle" function. IgA+GL7+ positive area percentage was calculated by applying the image Calculator "AND" function over IgA and GL7 masks, then measuring the resulting area by analyze particle function and calculating the percentage of the resulting area over the whole GL7 positive area.

In vitro plasma cell culture

All mice were injected retro orbitally with 1µg αCD45-BUV395 5 minutes prior to euthanasia. B cells from spleen, medLN or lung were isolated using negative magnetic bead separation (STEMCell). Cultures with R848 only were performed on lympholyte-M (Cedarlane) separated lung B cells and B cells from spleen isolated using negative magnetic bead separation. $B220^+$ B cells were then sorted for i.v. $CD45^-$ populations using an Aria FACS sorter (BD Biosciences). Plasma cells were differentiated from naive B cells. Briefly, cells were suspended in Iscove's modified Dulbecco's medium (IMDM, cytiva) supplemented with 10% FBS (Sigma), 2mM Glutamax (Gibco), 55µM β-mercaptoethanol (Gibco), 100U/mL penicillin (Gibco) and 100µg/mL streptomycin (Gibco) and activated with 1µg/mL CpG (Invivogen) for two days. Cells were then seeded over irradiated 40LB feeder cells, a generous gift from Dr. Daisuke Kitamura[30], expressing mouse CD40L and BAFF. To induce class switch to IgA, cells were incubated with 2ng/mL TGF-β (BioLegend), 100nM retinoic acid (RA, Sigma) and 40ng/mL IL-21 (Peprotech) for three days, followed by three days in IL-21 alone.

ELISA

Enzyme linked immunosorbent assays (ELISAs) were performed on the supernatant of cultured cells (see *in vitro* plasma cell culture for culture details). Immulon 2HB plates (ThermoFisher) were pre-coated with 2µg/mL of goat-α-mouse Ig(H+L) (Southern Biotech) diluted in PBS. Serial dilutions of supernatant were plated and left overnight at 4°C. The plates were developed using α-mouse IgA-AP Abs (Southern Biotech) followed by 4-Nitropenyl phosphate disodium salt hexahydrate substrate tablets (Sigma). Absorbance was measured using a Spectramax 190 luminometer (Molecular Devices) at 405 nm.

Statistical analysis

Raw data from control and cKO PR8-infected groups were analyzed by Mann-Whiney U test or 2-way ANOVA using GraphPad Prism (v.9.3.1). $p<0.05$ were considered statistically significant.

Acknowledgements

We thank Sara Sagadiev, Aaron Liu and Ursula Holder for laboratory assistance and useful insights and discussion. This research was supported by the Office of Animal Care, the Microscopy and Histopathology CoLab and the Flow Cytometry Core at Seattle Children's Research Institute.

Funding

This work was supported by National Institute of Health R01 AI151167 (to M.A.)

References

1. DeFranco AL, Rookhuizen DC, Hou B. Contribution of Toll-like receptor signaling to germinal center antibody responses. Immunol Rev. 2012;247(1):64-72. doi: 10.1111/j.1600-065X.2012.01115.x. PubMed PMID: 22500832; PMCID: PMC3334874.
2. Acharya M, Edkins AL, Ozanne BW, Cushley W. SDF-1 and PDGF enhance alphavbeta5-mediated ERK activation and adhesion-independent growth of human pre-B cell lines. Leukemia. 2009;23(10):1807-17. doi: 10.1038/leu.2009.126. PubMed PMID: 19609283.

3. Acharya M, Mukhopadhyay S, Paidassi H, Jamil T, Chow C, Kissler S, Stuart LM, Hynes RO, Lacy-Hulbert A. alphav Integrin expression by DCs is required for Th17 cell differentiation and development of experimental autoimmune encephalomyelitis in mice. J Clin Invest. 2010;120(12):4445-52. doi: 10.1172/JCI43796. PubMed PMID: 21099114; PMCID: PMC2993596.
4. Gianni T, Leoni V, Chesnokova LS, Hutt-Fletcher LM, Campadelli-Fiume G. alphavbeta3-integrin is a major sensor and activator of innate immunity to herpes simplex virus-1. Proc Natl Acad Sci U S A. 2012;109(48):19792-7. doi: 10.1073/pnas.1212597109. PubMed PMID: 23150579; PMCID: PMC3511702.
5. Lacy-Hulbert A, Smith AM, Tissire H, Barry M, Crowley D, Bronson RT, Roes JT, Savill JS, Hynes RO. Ulcerative colitis and autoimmunity induced by loss of myeloid alphav integrins. Proc Natl Acad Sci U S A. 2007;104(40):15823-8. Epub 2007/09/27. doi: 10.1073/pnas.0707421104. PubMed PMID: 17895374; PMCID: PMC1994135.
6. Lucas M, Stuart LM, Savill J, Lacy-Hulbert A. Apoptotic cells and innate immune stimuli combine to regulate macrophage cytokine secretion. J Immunol. 2003;171(5):2610-5. Epub 2003/08/21. doi: 10.4049/jimmunol.171.5.2610. PubMed PMID: 12928413.
7. Overstreet MG, Gaylo A, Angermann BR, Hughson A, Hyun YM, Lambert K, Acharya M, Billroth-Maclurg AC, Rosenberg AF, Topham DJ, Yagita H, Kim M, Lacy-Hulbert A, Meier-Schellersheim M, Fowell DJ. Inflammation-induced interstitial migration of effector CD4(+) T cells is dependent on integrin alphaV. Nat Immunol. 2013;14(9):949-58. doi: 10.1038/ni.2682. PubMed PMID: 23933892; PMCID: PMC4159184.
8. Savill J, Dransfield I, Hogg N, Haslett C. Vitronectin receptor-mediated phagocytosis of cells undergoing apoptosis. Nature. 1990;343(6254):170-3. doi: 10.1038/343170a0. PubMed PMID: 1688647.
9. Schrock DC, Leddon SA, Hughson A, Miller J, Lacy-Hulbert A, Fowell DJ. Pivotal role for alphaV integrins in sustained Tfh support of the germinal center response for long-lived plasma cell generation. Proc Natl Acad Sci U S A. 2019. doi: 10.1073/pnas.1809329116. PubMed PMID: 30770452; PMCID: PMC6410787.
10. Acharya M, Sokolovska A, Tam JM, Conway KL, Stefani C, Raso F, Mukhopadhyay S, Feliu M, Paul E, Savill J, Hynes RO, Xavier RJ, Vyas JM, Stuart LM, Lacy-Hulbert A. alphav Integrins combine with LC3 and atg5 to regulate Toll-like receptor signalling in B cells. Nat Commun. 2016;7:10917. doi: 10.1038/ncomms10917. PubMed PMID: 26965188; PMCID: PMC4792966.
11. Raso F, Sagadiev S, Du S, Gage E, Arkatkar T, Metzler G, Stuart LM, Orr MT, Rawlings DJ, Jackson SW, Lacy-Hulbert A, Acharya M. alphav Integrins regulate germinal center B cell responses through noncanonical autophagy. J Clin Invest. 2018;128(9):4163-78. Epub 2018/07/13. doi: 10.1172/JCI99597. PubMed PMID: 29999501; PMCID: PMC6118577.
12. Muir V, Sagadiev S, Liu S, Holder U, Armendariz AM, Suchland E, Meitlis I, Camp N, Giltiay N, Tam JM, Garner EC, Wivagg CN, Shows D, James RG, Lacy-Hulbert A, Acharya M. Transcriptomic analysis of pathways associated with ITGAV/alpha(v) integrin-dependent autophagy in human B cells. Autophagy. 2023;19(3):926-42. Epub 20220825. doi: 10.1080/15548627.2022.2113296. PubMed PMID: 36016494.
13. Acharya M, Raso F, Sagadiev S, Gilbertson E, Kadavy L, Li QZ, Yan M, Stuart LM, Hamerman JA, Lacy-Hulbert A. B Cell alphav Integrins Regulate TLR-Driven Autoimmunity. J Immunol. 2020;205(7):1810-8. Epub 2020/08/30. doi: 10.4049/jimmunol.1901056. PubMed PMID: 32859730; PMCID: PMC7504890.
14. Allie SR, Bradley JE, Mudunuru U, Schultz MD, Graf BA, Lund FE, Randall TD. The establishment of resident memory B cells in the lung requires local antigen encounter. Nat Immunol. 2019;20(1):97-108. Epub 2018/12/05. doi: 10.1038/s41590-018-0260-6. PubMed PMID: 30510223; PMCID: PMC6392030.

15. Oh JE, Song E, Moriyama M, Wong P, Zhang S, Jiang R, Strohmeier S, Kleinstein SH, Krammer F, Iwasaki A. Intranasal priming induces local lung-resident B cell populations that secrete protective mucosal antiviral IgA. Sci Immunol. 2021;6(66):eabj5129. Epub 20211210. doi: 10.1126/sciimmunol.abj5129. PubMed PMID: 34890255; PMCID: PMC8762609.
16. Kadaoui KA, Corthesy B. Secretory IgA mediates bacterial translocation to dendritic cells in mouse Peyer's patches with restriction to mucosal compartment. J Immunol. 2007;179(11):7751-7. doi: 10.4049/jimmunol.179.11.7751. PubMed PMID: 18025221.
17. Kaetzel CS, Robinson JK, Chintalacharuvu KR, Vaerman JP, Lamm ME. The polymeric immunoglobulin receptor (secretory component) mediates transport of immune complexes across epithelial cells: a local defense function for IgA. Proc Natl Acad Sci U S A. 1991;88(19):8796-800. doi: 10.1073/pnas.88.19.8796. PubMed PMID: 1924341; PMCID: PMC52597.
18. Kaetzel CS, Robinson JK, Lamm ME. Epithelial transcytosis of monomeric IgA and IgG cross-linked through antigen to polymeric IgA. A role for monomeric antibodies in the mucosal immune system. J Immunol. 1994;152(1):72-6. PubMed PMID: 8254208.
19. Mbawuike IN, Pacheco S, Acuna CL, Switzer KC, Zhang Y, Harriman GR. Mucosal immunity to influenza without IgA: an IgA knockout mouse model. J Immunol. 1999;162(5):2530-7. PubMed PMID: 10072492.
20. Renegar KB, Small PA, Jr. Passive transfer of local immunity to influenza virus infection by IgA antibody. J Immunol. 1991;146(6):1972-8. PubMed PMID: 2005388.
21. Tamura S, Funato H, Hirabayashi Y, Suzuki Y, Nagamine T, Aizawa C, Kurata T. Cross-protection against influenza A virus infection by passively transferred respiratory tract IgA antibodies to different hemagglutinin molecules. Eur J Immunol. 1991;21(6):1337-44. doi: 10.1002/eji.1830210602. PubMed PMID: 1646112.
22. Meyer-Bahlburg A. B-1 cells as a source of IgA. Ann N Y Acad Sci. 2015;1362:122-31. Epub 20150609. doi: 10.1111/nyas.12801. PubMed PMID: 26062045.
23. de Carvalho RVH, Ersching J, Barbulescu A, Hobbs A, Castro TBR, Mesin L, Jacobsen JT, Phillips BK, Hoffmann HH, Parsa R, Canesso MCC, Nowosad CR, Feng A, Leist SR, Baric RS, Yang E, Utz PJ, Victora GD. Clonal replacement sustains long-lived germinal centers primed by respiratory viruses. Cell. 2023;186(1):131-46 e13. Epub 20221223. doi: 10.1016/j.cell.2022.11.031. PubMed PMID: 36565697; PMCID: PMC9870066.
24. Kanekiyo M, Joyce MG, Gillespie RA, Gallagher JR, Andrews SF, Yassine HM, Wheatley AK, Fisher BE, Ambrozak DR, Creanga A, Leung K, Yang ES, Boyoglu-Barnum S, Georgiev IS, Tsybovsky Y, Prabhakaran MS, Andersen H, Kong WP, Baxa U, Zephir KL, Ledgerwood JE, Koup RA, Kwong PD, Harris AK, McDermott AB, Mascola JR, Graham BS. Mosaic nanoparticle display of diverse influenza virus hemagglutinins elicits broad B cell responses. Nat Immunol. 2019;20(3):362-72. Epub 20190211. doi: 10.1038/s41590-018-0305-x. PubMed PMID: 30742080; PMCID: PMC6380945.
25. Chen H, Lau MC, Wong MT, Newell EW, Poidinger M, Chen J. Cytofkit: A Bioconductor Package for an Integrated Mass Cytometry Data Analysis Pipeline. PLoS Comput Biol. 2016;12(9):e1005112. Epub 20160923. doi: 10.1371/journal.pcbi.1005112. PubMed PMID: 27662185; PMCID: PMC5035035.
26. Conter LJ, Song E, Shlomchik MJ, Tomayko MM. CD73 expression is dynamically regulated in the germinal center and bone marrow plasma cells are diminished in its absence. PLoS One. 2014;9(3):e92009. Epub 20140324. doi: 10.1371/journal.pone.0092009. PubMed PMID: 24664100; PMCID: PMC3963874.
27. Matsumoto R, Gray J, Rybkina K, Oppenheimer H, Levy L, Friedman LM, Khamaisi M, Meng W, Rosenfeld AM, Guyer RS, Bradley MC, Chen D, Atkinson MA, Brusko TM, Brusko M, Connors TJ, Luning Prak ET, Hershberg U, Sims PA, Hertz T, Farber DL. Induction of bronchus-associated lymphoid tissue is an early life adaptation for promoting human B cell immunity. Nat Immunol. 2023;24(8):1370-81.

Epub 20230717. doi: 10.1038/s41590-023-01557-3. PubMed PMID: 37460638; PMCID: PMC10529876.
28. Moyron-Quiroz JE, Rangel-Moreno J, Kusser K, Hartson L, Sprague F, Goodrich S, Woodland DL, Lund FE, Randall TD. Role of inducible bronchus associated lymphoid tissue (iBALT) in respiratory immunity. Nat Med. 2004;10(9):927-34. Epub 20040815. doi: 10.1038/nm1091. PubMed PMID: 15311275.
29. Hung KL, Meitlis I, Hale M, Chen CY, Singh S, Jackson SW, Miao CH, Khan IF, Rawlings DJ, James RG. Engineering Protein-Secreting Plasma Cells by Homology-Directed Repair in Primary Human B Cells. Mol Ther. 2018;26(2):456-67. Epub 2017/12/24. doi: 10.1016/j.ymthe.2017.11.012. PubMed PMID: 29273498; PMCID: PMC5835153.
30. Nojima T, Haniuda K, Moutai T, Matsudaira M, Mizokawa S, Shiratori I, Azuma T, Kitamura D. In-vitro derived germinal centre B cells differentially generate memory B or plasma cells in vivo. Nat Commun. 2011;2:465. Epub 20110906. doi: 10.1038/ncomms1475. PubMed PMID: 21897376.
31. Victora GD, Nussenzweig MC. Germinal centers. Annu Rev Immunol. 2012;30:429-57. doi: 10.1146/annurev-immunol-020711-075032. PubMed PMID: 22224772.
32. Corti D, Bianchi S, Vanzetta F, Minola A, Perez L, Agatic G, Guarino B, Silacci C, Marcandalli J, Marsland BJ, Piralla A, Percivalle E, Sallusto F, Baldanti F, Lanzavecchia A. Cross-neutralization of four paramyxoviruses by a human monoclonal antibody. Nature. 2013;501(7467):439-43. doi: 10.1038/nature12442. PubMed PMID: 23955151.
33. Pappas L, Foglierini M, Piccoli L, Kallewaard NL, Turrini F, Silacci C, Fernandez-Rodriguez B, Agatic G, Giacchetto-Sasselli I, Pellicciotta G, Sallusto F, Zhu Q, Vicenzi E, Corti D, Lanzavecchia A. Rapid development of broadly influenza neutralizing antibodies through redundant mutations. Nature. 2014;516(7531):418-22. doi: 10.1038/nature13764. PubMed PMID: 25296253.
34. Matz HC, McIntire KM, Ellebedy AH. 'Persistent germinal center responses: slow-growing trees bear the best fruits'. Curr Opin Immunol. 2023;83:102332. Epub 20230505. doi: 10.1016/j.coi.2023.102332. PubMed PMID: 37150126; PMCID: PMC10829534.
35. Tan HX, Esterbauer R, Vanderven HA, Juno JA, Kent SJ, Wheatley AK. Inducible Bronchus-Associated Lymphoid Tissues (iBALT) Serve as Sites of B Cell Selection and Maturation Following Influenza Infection in Mice. Front Immunol. 2019;10:611. Epub 20190329. doi: 10.3389/fimmu.2019.00611. PubMed PMID: 30984186; PMCID: PMC6450362.
36. Tschernig T, Pabst R. Bronchus-Associated Lymphoid Tissue (BALT) Is Not Present in the Normal Adult Lung but in Different Diseases. Pathobiology. 2000:1-8.
37. Chiavolini D, Rangel-Moreno J, Berg G, Christian K, Oliveira-Nascimento L, Weir S, Alroy J, Randall TD, Wetzler LM. Bronchus-associated lymphoid tissue (BALT) and survival in a vaccine mouse model of tularemia. PLoS One. 2010;5(6):e11156. Epub 20100616. doi: 10.1371/journal.pone.0011156. PubMed PMID: 20585390; PMCID: PMC2886834.
38. Moyron-Quiroz JE, Rangel-Moreno J, Hartson L, Kusser K, Tighe MP, Klonowski KD, Lefrancois L, Cauley LS, Harmsen AG, Lund FE, Randall TD. Persistence and responsiveness of immunologic memory in the absence of secondary lymphoid organs. Immunity. 2006;25(4):643-54. doi: 10.1016/j.immuni.2006.08.022. PubMed PMID: 17045819.
39. Baumgarth N. How specific is too specific? B-cell responses to viral infections reveal the importance of breadth over depth. Immunol Rev. 2013;255(1):82-94. Epub 2013/08/21. doi: 10.1111/imr.12094. PubMed PMID: 23947349; PMCID: PMC3748619.
40. MacLean AJ, Richmond N, Koneva L, Attar M, Medina CAP, Thornton EE, Gomes AC, El-Turabi A, Bachmann MF, Rijal P, Tan TK, Townsend A, Sansom SN, Bannard O, Arnon TI. Secondary influenza challenge triggers resident memory B cell migration and rapid relocation to boost antibody secretion at infected sites. Immunity. 2022;55(4):718-33 e8. Epub 20220328. doi: 10.1016/j.immuni.2022.03.003. PubMed PMID: 35349789; PMCID: PMC9044924.

41. Onodera T, Takahashi Y, Yokoi Y, Ato M, Kodama Y, Hachimura S, Kurosaki T, Kobayashi K. Memory B cells in the lung participate in protective humoral immune responses to pulmonary influenza virus reinfection. Proc Natl Acad Sci U S A. 2012;109(7):2485-90. doi: 10.1073/pnas.1115369109. PubMed PMID: 22308386; PMCID: PMC3289300.
42. Macpherson AJ, McCoy KD, Johansen FE, Brandtzaeg P. The immune geography of IgA induction and function. Mucosal Immunol. 2008;1(1):11-22. doi: 10.1038/mi.2007.6. PubMed PMID: 19079156.
43. Reboldi A, Arnon TI, Rodda LB, Atakilit A, Sheppard D, Cyster JG. IgA production requires B cell interaction with subepithelial dendritic cells in Peyer's patches. Science. 2016;352(6287):aaf4822. doi: 10.1126/science.aaf4822. PubMed PMID: 27174992; PMCID: PMC4890166.
44. Okuya K, Yoshida R, Manzoor R, Saito S, Suzuki T, Sasaki M, Saito T, Kida Y, Mori-Kajihara A, Kondoh T, Sato M, Kajihara M, Miyamoto H, Ichii O, Higashi H, Takada A. Potential Role of Nonneutralizing IgA Antibodies in Cross-Protective Immunity against Influenza A Viruses of Multiple Hemagglutinin Subtypes. J Virol. 2020;94(12). Epub 20200601. doi: 10.1128/JVI.00408-20. PubMed PMID: 32269119; PMCID: PMC7307104.
45. Hassan AO, Kafai NM, Dmitriev IP, Fox JM, Smith BK, Harvey IB, Chen RE, Winkler ES, Wessel AW, Case JB, Kashentseva E, McCune BT, Bailey AL, Zhao H, VanBlargan LA, Dai YN, Ma M, Adams LJ, Shrihari S, Danis JE, Gralinski LE, Hou YJ, Schafer A, Kim AS, Keeler SP, Weiskopf D, Baric RS, Holtzman MJ, Fremont DH, Curiel DT, Diamond MS. A Single-Dose Intranasal ChAd Vaccine Protects Upper and Lower Respiratory Tracts against SARS-CoV-2. Cell. 2020;183(1):169-84 e13. Epub 20200819. doi: 10.1016/j.cell.2020.08.026. PubMed PMID: 32931734; PMCID: PMC7437481.
46. Hassan AO, Shrihari S, Gorman MJ, Ying B, Yuan D, Raju S, Chen RE, Dmitriev IP, Kashentseva E, Adams LJ, Mann C, Davis-Gardner ME, Suthar MS, Shi PY, Saphire EO, Fremont DH, Curiel DT, Alter G, Diamond MS. An intranasal vaccine durably protects against SARS-CoV-2 variants in mice. Cell Rep. 2021;36(4):109452. Epub 20210710. doi: 10.1016/j.celrep.2021.109452. PubMed PMID: 34289385; PMCID: PMC8270739.
47. Gage E, Van Hoeven N, Dubois Cauwelaert N, Larsen SE, Erasmus J, Orr MT, Coler RN. Memory CD4(+) T cells enhance B-cell responses to drifting influenza immunization. Eur J Immunol. 2019;49(2):266-76. Epub 2018/12/15. doi: 10.1002/eji.201847852. PubMed PMID: 30548475; PMCID: PMC6494461.
48. Davenport ML, Sherrill TP, Blackwell TS, Edmonds MD. Perfusion and Inflation of the Mouse Lung for Tumor Histology. J Vis Exp. 2020(162). Epub 20200806. doi: 10.3791/60605. PubMed PMID: 32831298; PMCID: PMC7877253.
49. Schindelin J, Arganda-Carreras I, Frise E, Kaynig V, Longair M, Pietzsch T, Preibisch S, Rueden C, Saalfeld S, Schmid B, Tinevez JY, White DJ, Hartenstein V, Eliceiri K, Tomancak P, Cardona A. Fiji: an open-source platform for biological-image analysis. Nat Methods. 2012;9(7):676-82. Epub 20120628. doi: 10.1038/nmeth.2019. PubMed PMID: 22743772; PMCID: PMC3855844.

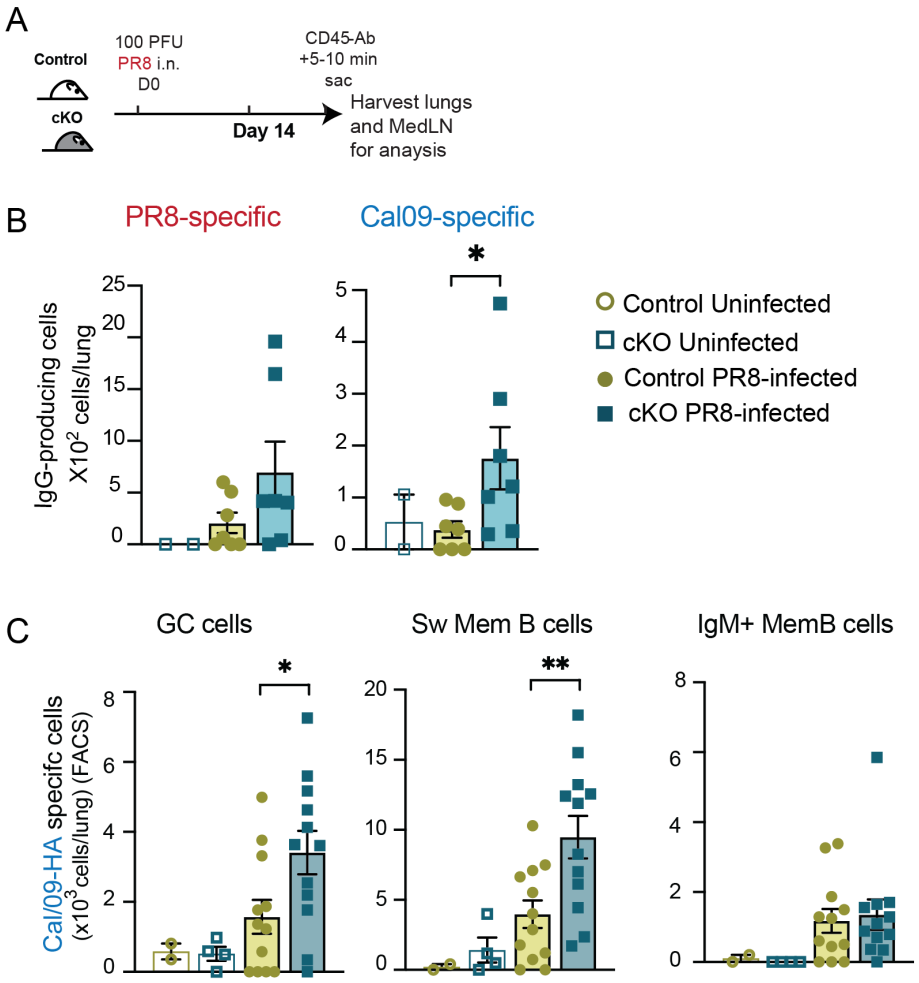

Figure 1. *Generation of cross-reactive B cell responses in the lungs is regulated by B cell αv integrin.* $\alpha v^{+/+}$ $CD19^{Cre+}$ (control) and $\alpha v^{fl/fl}$ $CD19^{Cre+}$ (cKO) mice were infected i.n. with 100 plaque-forming units (PFU) gof live PR8 IAV. 14 days later all mice received a retro-orbital (r.o.) injection with 1µg anti-CD45 antibody (Ab) (α-CD45-BUV395) five minutes prior to euthanasia. (**A**) Schematic for experimental procedure. (**B**) IgG-secreting cells in the lung that recognize either PR8-HA or Cal09-HA enumerated by ELISpot. Cells per lung were calculated by multiplying the frequency of live cells by the total number of live lymphocytes counted. (**C**) Antigen-specific germinal center (GC, left), class-switched memory B cells (Sw Mem B cells, middle) and IgM+ memory B cells (right) from the lung were enumerated by flow cytometry from the i.v. $CD45^-$ population (see Supplemental **Figure 1** for gating strategy). Cells were first gated as live lung-resident cells (i.v. CD45-unlabeled) and Plasma cells (PCs) were gated as IgD- IRF4+ CD138+ cells. B cells were gated as CD19 and CD138 (CD19+ CD138+/-), IgD+ cells were excluded from the analysis, germinal center cells (GCs) were gated as IgD- IRF4- CD138- Fas+ PNA+ and Sw memory B cells were gated as IgD- IRF4- CD138- Fas- PNA- IgM- IgA-. Cells per lung were calculated by multiplying the frequency of each population, as determined by flow cytometry, by the number of total live cells recovered from the tissue harvest. Each dot represents an individual mouse (n= 2-4 mice for uninfected group and n=7-12 mice for infected groups). Data are means ± SEM either representative experiment from 3 independent experiment (**B**) or the combination (**C**) of two independent experiments. *p<0.05, **p<0.01 by Mann-Whitney U-test between the two PR8-infected groups.

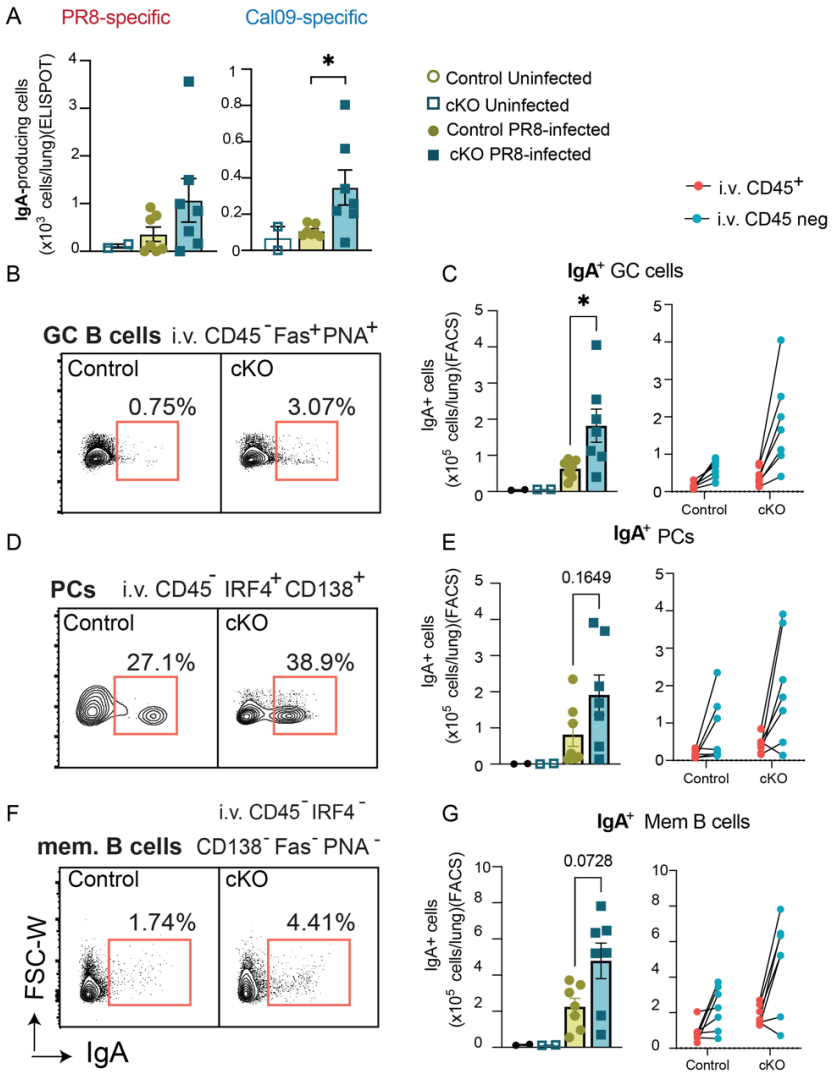

Figure 2. *Absence of B cell αv integrin promotes IgA B cell response in the lungs after influenza infection.* $\alpha v^{+/+}$ $CD19^{Cre+}$ (control) and $\alpha v^{fl/fl}$ $CD19^{Cre+}$ (cKO) mice were infected i.n. with 100 plaque-forming units (PFU) of live H1N1 PR8 IAV. After 14 days of infection all mice received r.o. injection with 1µg α-CD45-BUV395 five minutes prior to euthanasia. (**A**) IgA-secreting cells in the lungs that recognize PR8-HA (left) or Cal09-HA (right) as detected by ELISPOT. Cells per lungs were calculated by multiplying the frequency of live cells by the total number of live lymphocytes counted. (**B-F**) Representative flow plots of the expression of IgA on GC B cells (top), PCs (middle) and mem B cells (bottom) (See Supplemental **Figure 1** for gating strategies) are shown in (**B**) (**D**) and **(F)**. Live lung-resident cells (i.v. CD45-) were gated on CD19 and CD138 to identify B cells (CD19+ CD138+/-), IgD+ cells were excluded from the analysis. Plasma cells (PCs) were gated as IgD- IRF4+ CD138+, germinal center cells (GCs) were gated as IgD- IRF4- CD138- Fas+ PNA+ and IgA memory B cells were gated as IgD- IRF4- CD138- Fas- PNA- IgM- IgA+. Quantification from flow analysis is shown in (**C**) (**E**) and (**G**). Cells per lung for IgA+ GCs (**C**), IgA+ PCs (**E**) and IgA Memory B cells (**G**) is shown in the control and cKO, uninfected and infected mice (left) and the frequency of each population comparing the cell number of resident (CD45- unlabeled) vs circulating (CD45-labeled) cells in the control and cKO mice (right). Each dot represents an individual mouse (n= 2mice for uninfected group and n=6-7 mice for infected groups). Data are means ± SEM from one representative experiment from 3 independent experiments. *p<0.05 by Mann-Whitney U-test between the two PR8-infected groups.

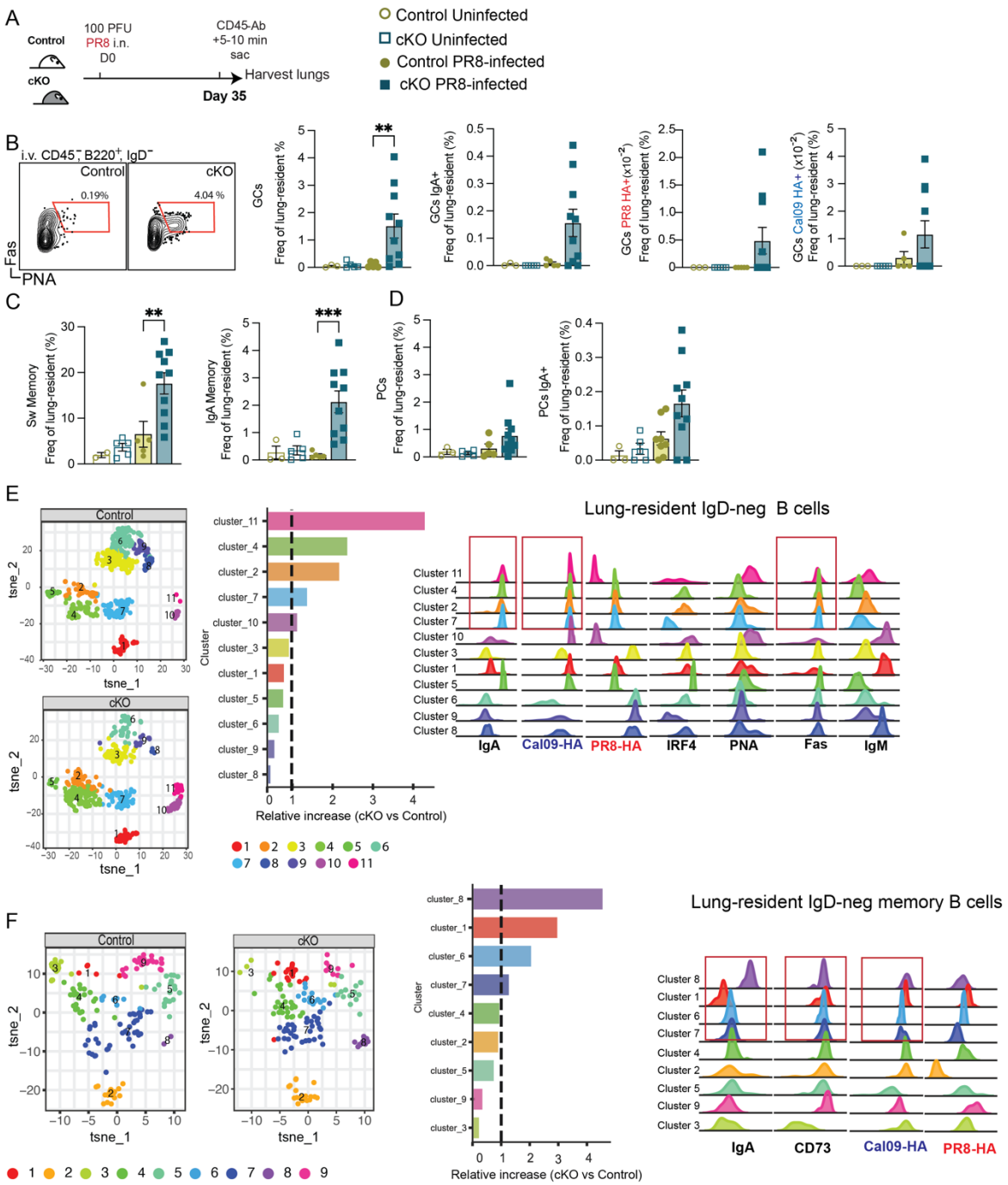

Figure 3. *Absence of B cell αv integrin leads to sustained increase in cross-reactive IgA+ GC and memory B cells in the lungs.* $\alpha v^{+/+}$ $CD19^{Cre+}$ (control) and $\alpha v^{fl/fl}$ $CD19^{Cre+}$ (cKO) mice were infected i.n. with 100 plaque-forming units (PFU) of live PR8 IAV. After 35 days of infection, all mice were injected r.o. with 1µg α-CD45-APC five minutes prior to euthanasia. (**A**) Schematic for experimental procedure. (**B**) Representative flow plot of the lung-resident germinal center cells (GC: B220+ IgD- IRF4- Fas+ PNA+) from a control and cKO mice at 35 days post infection. To the right, plots of the frequency of lung-resident (i.v CD45 negative) GCs, GCs IgA+, GCs PR8-HA+ and GCs Cal09-HA+ cells is shown as determined by flow cytometry. (**C**) Frequency of the lung-resident (i.v CD45-) class-switched (Sw Memory) (B220+ IgD- IRF4- Fas- PNA- IgM- IgA-) and IgA+ Memory cells and (**D**) lung-resident plasma cells (PCs, B220+ IgD- IRF4+) and IgA+ plasma cells, as determined by flow cytometry. Each dot represents an individual mouse (n=3-5

mice for uninfected group and n=6-10 mice for infected groups). Data are mean ± SEM of two representative experiments combined from 4 independent experiments. *p<0.05, **p<0.01, ***p<0.001 by Mann-Whitney U-test between the two PR8-infected groups. (**E**) t-SNE plot of HA-specific lung-resident IgD- B cells (i.v CD45- B220+ IRF4+/- IgD- PR8-HA+/Cal09-HA+) from lungs of infected control (top) and cKO mice (bottom) with the PhenoGraph clusters (left). Fold increase of the cell proportion per cluster in the cKO vs the control mice (middle). Histograms of the expression of the markers included in the analysis for each cluster, red boxes include the clusters with an increased frequency in the cKO mice compared to the control (right). (**F**) Mice were infected i.n. with 100 plaque-forming units (PFU) of live PR8 IAV and re-challenged at day 31 with 50 PFU live PR8. All mice received r.o. injection with 1µg α-CD45-APC five minutes prior to euthanasia. t-SNE plot of lung-resident IgD- memory B cells (iv CD45- B220+ IRF4+/- IgD-, Fas- PNA-) from infected control (left) and cKO mice (right) with the PhenoGraph clusters. Fold increase of the cell proportion per cluster in the cKO vs the control mice (middle). Histograms of the expression of the markers included in the analysis for each cluster, red boxes include the clusters with an increased frequency in the cKO mice compared to the control (right). Analysis is based on n= 6 mice per group in both sets of cluster analysis.

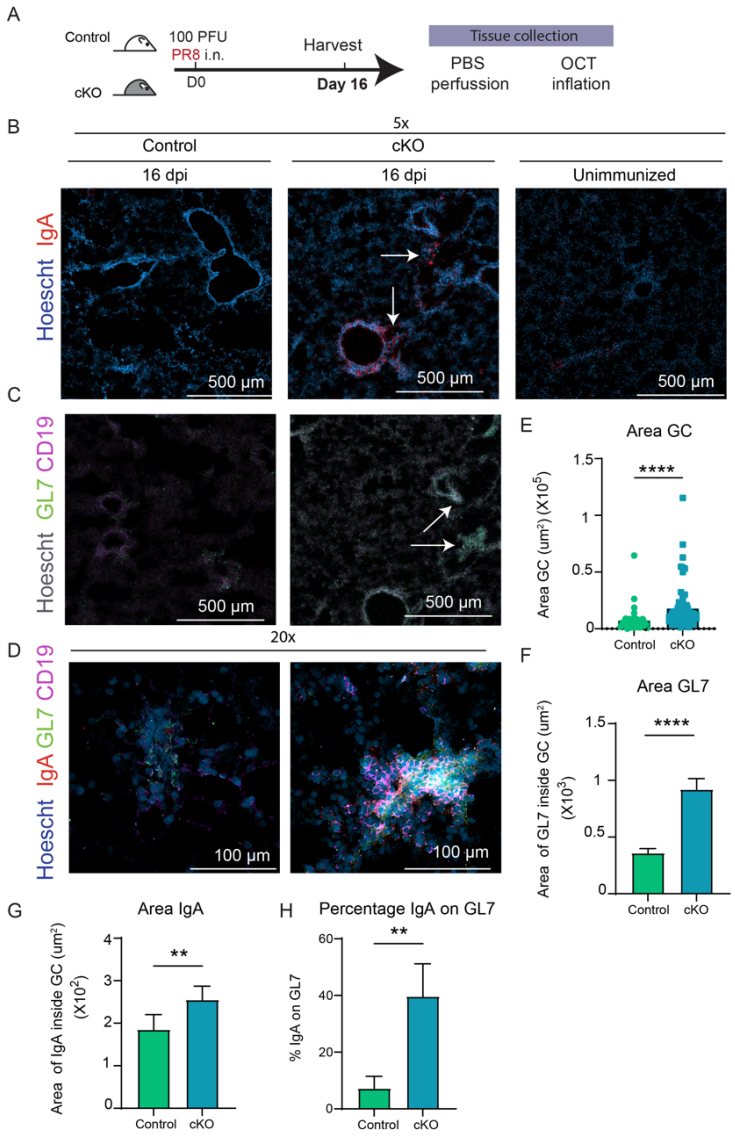

Figure 4. *Loss of B cell αv integrin enhances the induction of iBALT in lungs after viral infection.* $\alpha v^{+/+}$ $CD19^{Cre+}$ (control) and $\alpha v^{fl/fl}$ $CD19^{Cre+}$ (cKO) mice were infected i.n. with 100 plaque-forming units (PFU) of live PR8 IAV. Lungs were harvested after 16 days post infection (dpi). (**A**) Schematic of mice infection and tissue collection for lung tissue staining. (**B-C**) Representative confocal images of lungs from uninfected control mouse and infected control or cKO mice. Images representing one single plane at 5x magnification. Scale bar 500 µm. (**B**) Lung staining for Hoechst (nucleus, Blue) or IgA (red). Airways surrounded by IgA staining are shown by arrows. (**C**) Lung staining for Hoechst (nucleus, gray), GL7 (green), and CD19 (magenta). Arrows represent GL7 positive and CD19 positive structures corresponding to iBALTs. (**D**) Representative confocal images of lungs from control or cKO mice 16 dpi. Images representing one single plane at 20x magnification labeled with Hoechst (nucleus, Blue), IgA (red), GL7 (green), and CD19 (magenta) showing iBALTs. Scale bar 100 µm. (**E**) Scatter plot with a bar graph showing the average size (µm²) of GL7+CD19+ iBALT structures by manually quantifying the area of these structures. Every dot is the size of 1 iBALT structure (35-65 structures) from 22-28 different fields of sections viewed at 10x from 3 different mice per genotype. (**F and G**) Bar graph showing mean and SEM of the area (µm²) of (**F**) GL7 and (**G**) IgA positive staining inside the structures (N= 35-65) as defined in **E**. (**H**) Bar graph showing mean and SEM of the percentage of IgA+GL7+ staining within iBALT structures. Sections (N=7-9) viewed at 20x from 3 different mice per group. **p<0.01, ****p<0,0001 by Mann-Whitney U-test.

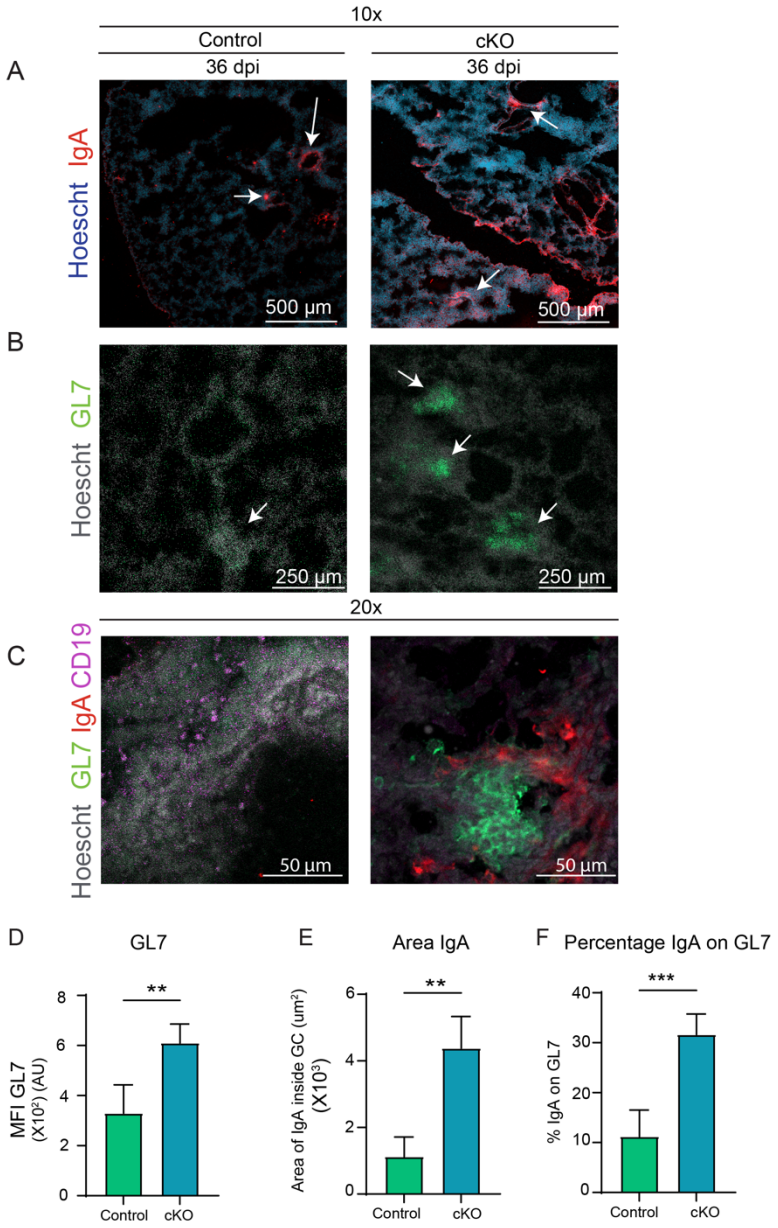

Figure 5: *Absence of αv B cell integrin leads to persistence of GC reactions in the lungs after influenza infection.* Mice were infected as in **Fig 4** and lungs were harvest at 36 days after PR8 IAV infection. (**A and B**) Representative confocal images of lungs from infected control or cKO mice at 10x magnification. Scale bar (**A**) 500 µm and (**B**) 250 µm. (**A**) Lung staining for Hoechst (nucleus, Blue) or IgA (red). IgA staining shown by arrows. (**B**) Lung staining for Hoechst (nucleus, gray) and GL7 (green). Arrows represent GL7 positive structures corresponding to iBALTs. (**C**) Representative confocal images of lungs from control or cKO mice of one single plane at 20x magnification labeled with Hoechst (nucleus, Blue), IgA (red), GL7 (green), and CD19 (magenta) showing iBALTs. Scale bar 50 µm. (**D**) Bar graph showing mean and SEM of the median fluorescence intensity of GL7 staining within the iBALT structures (N=12-27) from 9-12 different fields of sections viewed at 10x from 3 different mice per genotype. (**E and F**) Bar graph showing mean and SEM of the area (µm^2) (**E**) and percentage (**F**) of IgA positive staining inside the iBALT structures (N= 12-27) from 3 different mice per genotype. **p<0.01, ****p<0.0001 by Mann-Whitney U-test.

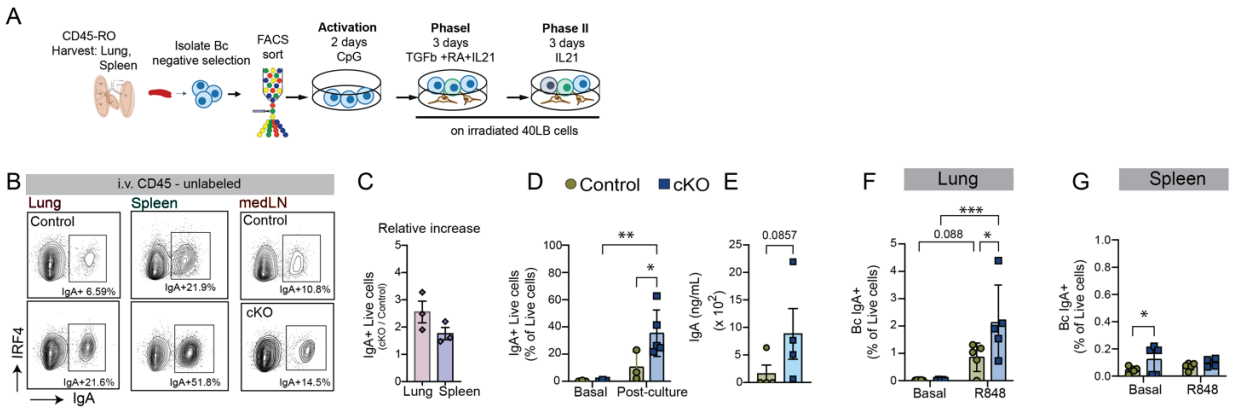

Figure 6: *B cell αv integrin regulates TLR signaling dependent IgA B cell differentiation.* C57BL/6 (control) and $\alpha v^{fl/fl}$ $CD19^{Cre+}$ (cKO) mice were injected r.o. with 1µg α-CD45-APC five minutes prior to euthanasia. Lung, spleen and medLN were then collected and sorted for i.v.CD45-unlabeled resident cells and plated for a total of 8 days. Cells were first activated with CpG for two days. Cells were then plated over 40LB feeder cells, expressing CD40L and BAFF, in the presence of TGFβ (2ng/mL), Retinoic acid (100nM) and IL-21 (40 ng/mL) for three days. Finally, the media was changed to fresh media containing only IL-21 for an additional three days. (**A**) Schematic of the experimental procedure. (**B**) Representative flow plots of lung, spleen and medLN resident B cells after the entire 8-day culture protocol. Cells were gated from live lymphocytes. (**C**) Relative increase in the frequency of IgA+ live cells, in the cKO vs the control cultures comparing cultures from lung and spleen B cells after the 8-day culture protocol. (**D**) Frequency of IgA-expressing live cells within lung-resident B cells after culture as determined by flow cytometry. (**E**) Secreted IgA as measured by ELISA of the supernatant of lung-resident B cells after TGFβ, RA and IL-21 culture. Each dot represents biological replicate from independent experiments. (**F and G**) Frequency of IgA-expressing B cells after 4 days of culture of (**F**) lung and (**G**) spleen B cells with R848 only without feeder layer, as determined by flow cytometry. Each dot represents culture with cells from individual mice from one representative experiment shown out of 2 independent experiments. Bar graphs show mean and SEM, *p<0.01, **p<0.001, ***p<0.0001 by Mann-Whitney U-test (E) or 2-way ANOVA (D, F and G).